

Coded Index Modulation for Non-DC-Biased OFDM in Multiple LED Visible Light Communication

S. P. Alaka, T. Lakshmi Narasimhan[†], and A. Chockalingam

Department of ECE, Indian Institute of Science, Bangalore 560012

[†] Presently with National Instruments Private Limited, Bangalore 560029

Abstract—Use of multiple light emitting diodes (LED) is an attractive way to increase spectral efficiency in visible light communications (VLC). A non-DC-biased OFDM (NDC OFDM) scheme that uses two LEDs has been proposed in the literature recently. NDC OFDM has been shown to perform better than other OFDM schemes for VLC like DC-biased OFDM (DCO OFDM) and asymmetrically clipped OFDM (ACO OFDM) in multiple LEDs settings. In this paper, we propose an efficient multiple LED OFDM scheme for VLC which uses *coded index modulation*. The proposed scheme uses two transmitter blocks, each having a pair of LEDs. Within each block, NDC OFDM signaling is done. The selection of which block is activated in a signaling interval is decided by information bits (i.e., index bits). In order to improve the reliability of the index bits at the receiver (which is critical because of high channel correlation in multiple LEDs settings), we propose to use coding on the index bits alone. We call the proposed scheme as CI-NDC OFDM (coded index NDC OFDM) scheme. Simulation results show that, for the same spectral efficiency, CI-NDC OFDM that uses LDPC coding on the index bits performs better than NDC OFDM.

Keywords – Multiple LED VLC, DCO OFDM, ACO OFDM, Flip OFDM, NDC OFDM, coded index modulation, LDPC.

I. INTRODUCTION

Optical wireless communication, where information is conveyed through optical radiations in free space in outdoor and indoor environments, is emerging as a promising complementary technology to RF wireless communication. While communication using infrared wavelengths has been in existence for quite some time [1],[2], more recent interest centers around indoor communication using visible light wavelengths [3],[4]. A major attraction in indoor visible light communication (VLC) is the potential to simultaneously provide both energy-efficient lighting as well as high-speed short-range communication using inexpensive high-luminance light-emitting diodes (LED). Several other advantages including no RF radiation hazard, abundant VLC spectrum at no cost, and very high data rates make VLC increasingly popular.

Orthogonal frequency division multiplexing (OFDM) which is popular in both wired and wireless RF communications is attractive in VLC as well [5]. When OFDM is used in RF wireless communications, baseband OFDM signals in the complex domain are used to modulate the RF carrier. OFDM can be applied to VLC in context of intensity modulation and direct detection (IM/DD), where IM/DD is non-coherent and the transmit signal must be real and positive. This can be achieved by imposing Hermitian symmetry on the information symbols before the inverse fast Fourier transform (IFFT)

operation. Several papers have investigated OFDM in VLC [5]-[10], which have shown that OFDM is attractive in VLC systems. A 3 Gbps single-LED VLC link based on OFDM has been reported in [11].

Several techniques that generate VLC compatible OFDM signals in the positive real domain have been proposed in the literature [12]-[18]. These techniques include DC-biased optical (DCO) OFDM [12], asymmetrically clipped optical (ACO) OFDM [13]-[15], flip OFDM [16],[17], and non-DC biased (NDC) OFDM [18]. In the above works, DCO OFDM, ACO OFDM, and flip OFDM are studied for single-LED systems. The NDC OFDM in [18] uses two LEDs. In [18], it has been that NDC OFDM performs better compared with DCO OFDM and ACO OFDM that use two LEDs.

Use of multiple LEDs is a natural and attractive means to achieve increased spectral efficiencies in VLC. Our study in this paper focuses on multiple LED OFDM techniques to VLC. Our new contribution is the proposal of a scheme which brings in the advantage of ‘spatial indexing’ to OFDM schemes for VLC. In particular, we propose a ‘*indexed NDC (I-NDC) OFDM*’ scheme, where information bits are not only conveyed through the modulation symbols sent on the active LED, but also through the index of the active LED. This brings in the benefit of higher rate and better performance. Our simulation results show that, for the same spectral efficiency, the proposed I-NDC OFDM outperforms NDC OFDM in the low-to-moderate SNR regime. This is because, to achieve the same spectral efficiency, I-NDC OFDM can use a smaller-sized QAM. However, in the high-SNR regime, NDC OFDM performs better. We find that this is because of the high error rates witnessed by the index bits in I-NDC OFDM due to high channel correlation in multiple LED settings. In order to alleviate this problem and improve the reliability of the index bits at the receiver, we propose to use coding on the index bits alone. This proposed scheme is called ‘*coded I-NDC OFDM (CI-NDC OFDM)*’ scheme. Our simulation results show that, for the same spectral efficiency, the proposed CI-NDC OFDM with LDPC coding on the index bits performs better than NDC OFDM in VLC systems.

The remainder of this paper is organized as follows. Section II gives an overview of DCO OFDM, ACO OFDM, flip OFDM, and NDC OFDM schemes. The proposed CI-NDC OFDM and performance results and discussions are presented in Section III. Conclusions are presented in Section IV.

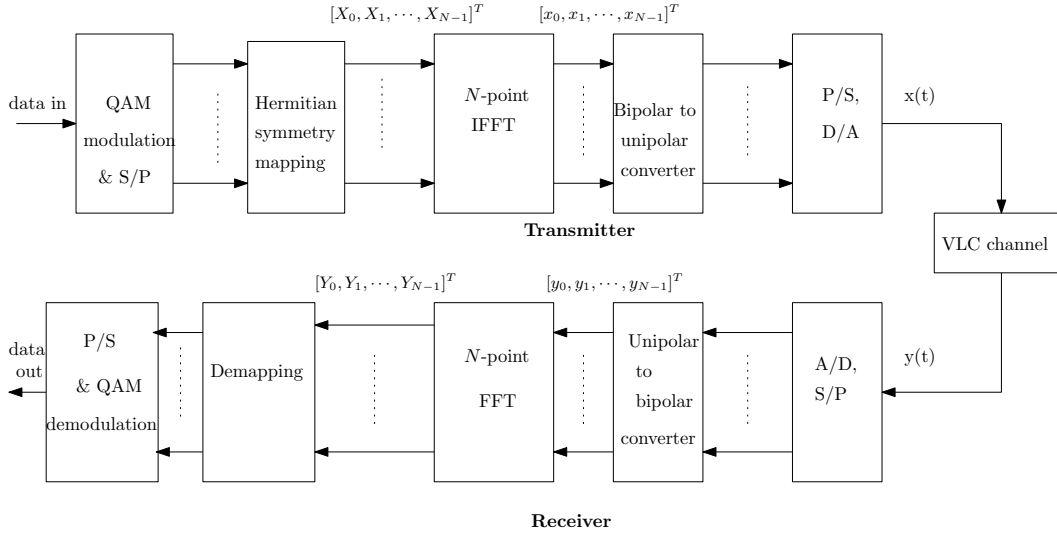


Fig. 1. A general single-LED OFDM system model in VLC.

II. OFDM SCHEMES FOR VLC

Here, we present an overview of the existing OFDM schemes for VLC reported in the literature. Figure 1 shows the block diagram of a general single-LED OFDM system with N subcarriers for VLC. In this system, a real OFDM signal is generated by constraining the input vector to the transmit N -point IFFT to have Hermitian symmetry, so that the output of the IFFT will be real. The output of the IFFT, though real, can be positive or negative. It can be made positive by several methods, namely, 1) adding DC bias (DCO OFDM [12]), 2) clipping at zero and transmitting only positive part (ACO OFDM [13]-[15]), and 3) transmitting both positive and negative parts after flipping the negative part (flip OFDM [16]). While the block diagram in Fig. 1 is for OFDM for VLC in general, the transmit and receive processing and achieved rates in bits per channel use (bpcu) can differ in the OFDM schemes listed above. These are highlighted below.

A. DCO OFDM

In DCO OFDM, $(\frac{N}{2} - 1) \log_2 M$ incoming data bits are mapped to $(\frac{N}{2} - 1)$ QAM symbols, where M is the QAM constellation size. The DC subcarrier (i.e., X_0) is set to zero. The $(\frac{N}{2} - 1)$ QAM symbols are mapped to subcarriers 1 to $(\frac{N}{2} - 1)$, i.e., $\{X_1, X_2, \dots, X_{\frac{N}{2}-1}\}$. Hermitian symmetry is applied to the remaining $\frac{N}{2}$ subcarriers, i.e., complex conjugates of the symbols on the first $\frac{N}{2}$ subcarriers are mapped on the second half subcarriers in the reverse order, where the $(\frac{N}{2} + 1)$ th subcarrier is set to zero. That is, the input to the N -point IFFT is given by

$$[0, X_1, X_2, \dots, X_{\frac{N}{2}-1}, 0, X_{\frac{N}{2}-1}^*, \dots, X_2^*, X_1^*]^T.$$

This Hermitian symmetry ensures that the IFFT output will be real and bipolar. These bipolar OFDM symbols $x(n)$, $n = 0, 1, \dots, N-1$, at the IFFT output are converted into unipolar by adding a DC bias, B_{dc} . Let $x(t)$ be the bipolar OFDM

signal without DC bias. Then the unipolar OFDM signal $x_{dc}(t)$ that drives the transmit LED is given by

$$x_{dc}(t) = x(t) + B_{dc},$$

where $B_{dc} = k\sqrt{\mathbb{E}\{x^2(t)\}}$. We define this as a bias of $10 \log_{10}(k^2+1)$ dB. Note that $k = 0$ corresponds to the case of no DC bias. For the DC bias to be not excessive, the negative going signal peaks must be clipped at zero. The performance of DCO OFDM depends on the amount of DC bias, which depends upon the size of the signal constellation [14]. For example, large QAM constellations require high SNRs for acceptable BERs, and therefore the clipping noise must be kept low, which, in turn, requires the DC bias to be large. As the DC bias increases, the required transmit power also increases. This makes the system power inefficient.

Due to Hermitian symmetry, the number of independent QAM symbols transmitted per OFDM symbol is reduced from N to $\frac{N}{2} - 1$. Thus, the achieved rate in DCO OFDM is

$$\eta_{dco} = \frac{N-2}{2N} \log_2 M \text{ bpcu.} \quad (1)$$

At the receiver side, the output of the photo detector (PD), $y(t)$, is digitized using an analog-to-digital converter (ADC) and the resulting sequence, $y(n)$, is processed further. The DC bias is first removed and the sequence after DC bias removal is fed as input to the N -point FFT. The FFT output sequence is $[Y_0, Y_1, \dots, Y_{N-1}]^T$. Only $\{Y_1, Y_2, \dots, Y_{\frac{N}{2}-1}\}$ in the FFT output need to be demapped and demodulated to recover the transmit data.

B. ACO OFDM

ACO OFDM does not use DC bias to convert the bipolar OFDM signal to unipolar. Instead, all negative values in the bipolar signal are clipped to zero. Clipping is a simpler operation in terms of implementation compared to DC bias. But this can introduce clipping noise. The effect of clipping

noise can be alleviated significantly by sending data symbols only on the odd subcarriers. More specifically, if only the odd subcarriers are used, the intermodulation product terms generated due to clipping fall on the even subcarriers, which are ignored. While this addresses the clipping noise issue, the achieved data rate is compromised by a factor of two compared to DCO OFDM, i.e., in an N -subcarrier ACO OFDM scheme, only $\frac{N}{4}$ subcarriers are used for data transmission, whereas DCO OFDM uses $\frac{N}{2} - 1$ subcarriers for data transmission.

In ACO OFDM, $\frac{N}{4} \log_2 M$ incoming bits are mapped to $\frac{N}{4} M$ -QAM symbols. These symbols are mapped on the first $\frac{N}{4}$ odd subcarriers. The even subcarriers are set to zero. To ensure Hermitian symmetry, the complex conjugates of the symbols on the first $\frac{N}{2}$ subcarriers are mapped on the remaining subcarriers in the reverse order, i.e., the input to the N -point IFFT is given by

$$[0, X_1, 0, X_2, 0, \dots, X_{\frac{N}{4}}, 0, X_{\frac{N}{4}}^*, \dots, 0, X_2^*, 0, X_1^*]^T.$$

The real bipolar signal at the IFFT output is then converted to unipolar by clipping the signal at zero. Let $x(n)$, $n = 0, 1, \dots, N - 1$, be the bipolar IFFT output signal. The unipolar signal is obtained as

$$s(n) = \begin{cases} x(n), & \text{if } x(n) > 0 \\ 0, & \text{if } x(n) \leq 0, \end{cases}$$

which drives the transmit LED after D/A conversion. Since only $\frac{N}{4}$ subcarriers among the N subcarriers are used to carry data, the achieved data rate in ACO OFDM is given by

$$\eta_{aco} = \frac{1}{4} \log_2 M \text{ bpcu.} \quad (2)$$

At the receiver side, the received signal $y(t)$ is first digitized to get $y(n)$, $n = 0, 1, \dots, N - 1$. This sequence is input to the N -point FFT. From the N -point FFT output, we take only the first $\frac{N}{4}$ odd subcarrier data, i.e., $\{Y_1, Y_3, \dots, Y_{\frac{N}{2}-1}\}$, and demodulate them to recover the transmit data.

C. Flip OFDM

Flip OFDM is similar to DCO OFDM except DC biasing. Instead of DC biasing, it uses two OFDM symbols to send the bipolar signals, i.e., positive and negative parts are sent as two consecutive OFDM symbols. Like in DCO OFDM, in flip OFDM also, the input to the N -point IFFT is

$$[0, X_1, X_2, \dots, X_{\frac{N}{2}-1}, 0, X_{\frac{N}{2}-1}^*, \dots, X_2^*, X_1^*]^T.$$

Let $x(n)$, $n = 0, 1, \dots, N - 1$, be the bipolar N -point IFFT output. The IFFT output $x(n)$ is fed to a polarity separator, which separates the positive and negative parts of $x(n)$. That is, the sequence $x(n)$ can be written in the form

$$x(n) = x^+(n) + x^-(n),$$

where

$$x^+(n) = \begin{cases} x(n), & \text{if } x(n) \geq 0 \\ 0, & \text{if } x(n) < 0 \end{cases}, \quad (3)$$

$$x^-(n) = \begin{cases} x(n), & \text{if } x(n) < 0 \\ 0, & \text{if } x(n) \geq 0. \end{cases} \quad (4)$$

The positive part $x^+(n)$ is transmitted as the first OFDM symbol. The polarity inverted (i.e., flipped) negative part (i.e., $-x^-(n)$) is transmitted as the second OFDM symbol. Note that the positive and negative parts of the bipolar OFDM signal are transmitted as two consecutive OFDM symbols with the negative part flipped. Since $(\frac{N}{2} - 1) M$ -QAM symbols are sent in two slots, the achieved data rate in flip OFDM is

$$\begin{aligned} \eta_{flip} &= \frac{\frac{N}{2} - 1}{2N} \log_2 M \\ &\approx \frac{1}{4} \log_2 M \text{ bpcu, for large } N. \end{aligned} \quad (5)$$

At the receiver, the received signal $y(t)$ is first digitized. Let $y^+(n)$ and $y^-(n)$ represent the time samples belonging to the first and second OFDM symbols, respectively. These two sample sequences are added; the polarity of the $y^-(n)$ is inverted before adding. Thus, the resulting bipolar signal $y(n)$ is given by $y(n) = y^+(n) - y^-(n)$, which is S/P converted and fed to the N -point FFT. The FFT output values of subcarriers 1 to $\frac{N}{2} - 1$ are demapped and demodulated to recover the transmit data.

D. NDC OFDM

NDC OFDM is similar to flip OFDM except the number of time slots used. Instead of sending the OFDM symbol in two consecutive time slots, this scheme exploits the spatial dimension. That is, this scheme uses two LEDs to send the bipolar signals; positive and negative parts drive two different LEDs. Figure 2 shows the block diagram of NDC OFDM. As in flip OFDM, the input to the N -point IFFT is given by

$$[0, X_1, X_2, \dots, X_{\frac{N}{2}-1}, 0, X_{\frac{N}{2}-1}^*, \dots, X_2^*, X_1^*]^T.$$

Let $x(n)$ be the bipolar IFFT output. As in flip OFDM, this output is fed to a polarity separator, which separates the positive and negative parts of $x(n)$, i.e., $x(n) = x^+(n) + x^-(n)$, where $x^+(n)$ and $x^-(n)$ are as defined in flip OFDM. $x^+(n)$ drives the first LED, and $-x^-(n)$ (i.e., flipped or polarity inverted signal) drives the second LED. Therefore, at a given time, only one LED will be active, where the index of the active LED (i.e., LED1 and LED2) is decided by the sign of the OFDM signal. This scheme can be viewed as OFDM with spatial modulation (SM), where the LED to activate in a given channel use is chosen based on the sign.

Due to Hermitian symmetry, the number of independent QAM symbols transmitted per OFDM symbol is reduced from N to $\frac{N}{2} - 1$. Thus, the achieved data rate of NDC OFDM is

$$\eta_{ndc} = \frac{N - 2}{2N} \log_2 M \text{ bpcu,} \quad (6)$$

which is the same as that of DCO OFDM.

The unipolar OFDM signal is transmitted over the VLC MIMO channel \mathbf{H} , where \mathbf{H} is a $N_r \times N_t$ channel matrix, N_t is the number of LEDs, and N_r is the number of PDs. Here, $N_t = N_r = 2$. The output of the PDs are fed to the ADCs. The digitized output of the ADCs, denoted by $\mathbf{y} = [y_1(n) \ y_2(n)]^T$, is fed as input to the SM detector. The SM detector, for

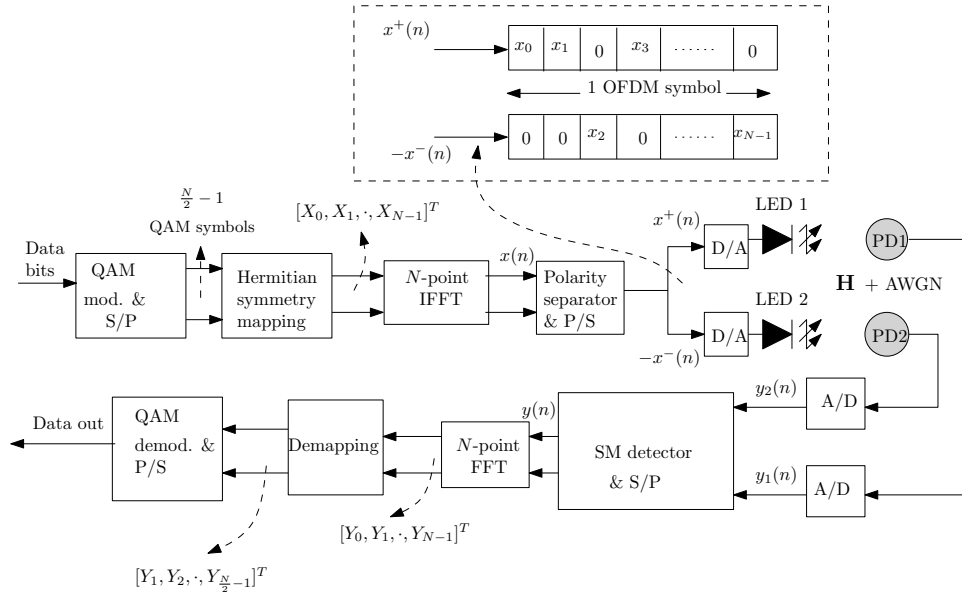


Fig. 2. Non-DC biased OFDM.

example, can be zero forcing (ZF) detector. That is, the SM detector output, denoted by $y(n)$, $n = 0, 1, \dots, N - 1$, is

$$|y(n)| = \max_{i=1,2} |z_i(n)|, \quad (7)$$

$$\text{sign}\{y(n)\} = \begin{cases} +\text{ve, if } \arg \max_{i=1,2} |z_i(n)| = 1 \\ -\text{ve, if } \arg \max_{i=1,2} |z_i(n)| = 2, \end{cases} \quad (8)$$

where

$$\begin{bmatrix} z_1(n) \\ z_2(n) \end{bmatrix} = \begin{bmatrix} (\mathbf{h}_1^T \mathbf{h}_1)^{-1} \mathbf{h}_1^T \mathbf{y} \\ (\mathbf{h}_2^T \mathbf{h}_2)^{-1} \mathbf{h}_2^T \mathbf{y} \end{bmatrix}, \quad (9)$$

and \mathbf{h}_i is the i th column of channel matrix \mathbf{H} , $i = 1, 2$. The SM detector output $y(n)$ is then fed to the N -point FFT. From the N -point FFT output, the subcarriers 1 to $(\frac{N}{2} - 1)$ are demodulated to get back the transmit data.

E. DCO/ACO/Flip/NDC OFDM performance comparison

Here, we illustrate a BER performance comparison between DCO OFDM, ACO OFDM, flip OFDM, and NDC OFDM. The indoor VLC system set up is shown in Fig. 3. The system parameters of the indoor VLC system considered in the simulation are given in Table I. All systems use $N_t = 2$ LEDs, $N_r = 2$ PDs. The PDs are kept symmetrical on top of a table with respect to the center of the floor with a d_{rx} of 0.1m. The LEDs are kept symmetrical with respect to the center of the room at 1m apart and at 3m height (i.e., $d_{tx} = 1$ m and $z = 3$ m). The channel gain between j th LED and i th PD is calculated as [2]

$$h_{ij} = \frac{n+1}{2\pi} \cos^n \phi_{ij} \cos \theta_{ij} \frac{A}{R_{ij}^2} \text{rect}\left(\frac{\theta_{ij}}{FOV}\right), \quad (10)$$

where ϕ_{ij} is the angle of emergence with respect to the j th source (LED) and the normal at the source, n is the mode

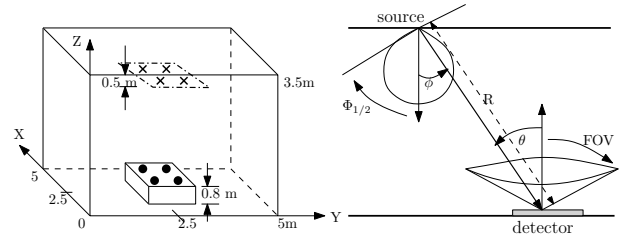


Fig. 3. Geometric set-up of the considered indoor VLC system. A dot represents a photo detector and a cross represents an LED.

Room	Length (X)	5m
	Width (Y)	5m
	Height (Z)	3.5m
Transmitter	Height from the floor	3m
	Elevation	-90°
	Azimuth	0°
	$\Phi_{1/2}$	60°
	Mode number, n	1
	d_{tx}	1m
Receiver	Height from the floor	0.8m
	Elevation	90°
	Azimuth	0°
	Responsivity, r	1 Ampere/Watt
	FOV	85°
	d_{rx}	0.1m

TABLE I
SYSTEM PARAMETERS IN THE CONSIDERED INDOOR VLC SYSTEM.

number of the radiating lobe given by $n = \frac{-\ln(2)}{\ln \cos \Phi_{1/2}}$, $\Phi_{1/2}$ is the half-power semiangle of the LED [19], θ_{ij} is the angle of incidence at the i th photo detector, A is the area of the detector, R_{ij} is the distance between the j th source and the i th detector, FOV is the field of view of the detector, and $\text{rect}(x) = 1$ if $|x| \leq 1$ and $\text{rect}(x) = 0$ if $|x| > 1$.

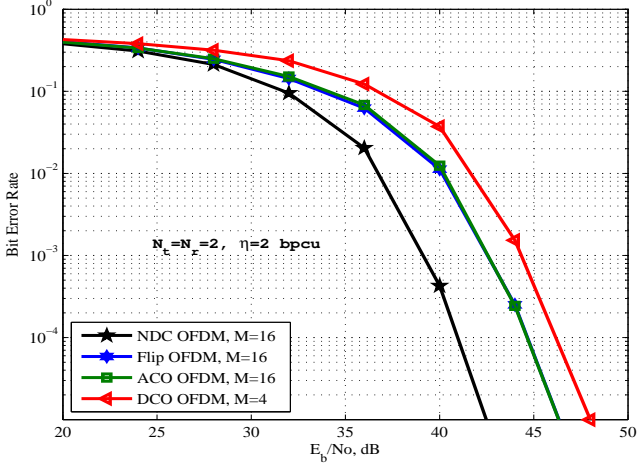


Fig. 4. Comparison of the BER performance of DCO OFDM, ACO OFDM, flip OFDM, and NDC OFDM $\eta = 2$ bpcu, $N_t = N_r = 2$.

Figure 4 shows the BER performance achieved by DCO OFDM, ACO OFDM, flip OFDM, and NDC OFDM for $\eta = 2$ bpcu, and $N_t = N_r = 2$. The parameters considered these systems are: 1) DCO OFDM: $N_t = N_r = 2$, $M = 4$, 7 dB bias, 2) ACO OFDM: $N_t = N_r = 2$, $M = 16$, 3) flip OFDM: $N_t = N_r = 2$, $M = 16$, and 4) NDC OFDM: $N_t = N_r = 2$, $M = 16$. In ACO OFDM, flip OFDM, and DCO OFDM, there are two parallel transmitting OFDM blocks, each drives one LED simultaneously. ZF detection is used for DCO OFDM, ACO OFDM, and flip OFDM. The hypothesis testing based detection method presented in Sec. II-D is used for NDC OFDM. From Fig. 4, it can be seen that DCO OFDM has poor performance compared to other systems, and this is due to the DC over-biasing. Also, ACO OFDM and flip OFDM have the same performance. Among the OFDM schemes discussed above, NDC OFDM achieves better performance compared to other OFDM schemes. This is because of the spatial interference experienced by the other OFDM schemes, i.e., while two LEDs are active simultaneously in DCO OFDM, ACO OFDM, and flip OFDM, only one LED will be active at a time in NDC OFDM.

III. PROPOSED CI-NDC OFDM FOR VLC

Motivated by the advantages of multiple LEDs and spatial indexing to achieve increased spectral efficiency, here we first propose a multiple LED OFDM scheme called ‘indexed NDC OFDM (I-NDC OFDM)’. In this scheme, additional bits are conveyed through the index of the active LED. Then, realizing the need to protect the index bits better in this scheme, we propose to use coding on the index bits. This scheme is called ‘coded index NDC OFDM (CI-NDC OFDM)’.

A. Proposed I-NDC OFDM

The block diagram of the proposed I-NDC OFDM transmitter is illustrated in Fig. 5. I-NDC OFDM is an N -subcarrier OFDM system with N_p pairs of LEDs and N_r photo detectors, where the total number of LEDs $N_t = 2N_p$. We consider $N_p = 2$, i.e., there are 2 pairs of LEDs. In

Fig. 5, the $\{LED1, LED2\}$ pair forms BLOCK 1 and the $\{LED3, LED4\}$ pair forms BLOCK 2. In each channel use, only one LED in either BLOCK 1 or BLOCK 2 will be activated. The choice of which BLOCK has to be activated in a given channel use is made based on indexing. In a general setting, m index bits can select one BLOCK among 2^m BLOCKS. In the considered system, $m = 1$ and $N_p = 2$. Therefore, the BLOCK selection is done using one index bit per channel use. The LED pair in the selected BLOCK will be driven as per the standard NDC OFDM scheme described in Sec. II-D. The I-NDC OFDM transmitter operation is described below.

Transmitter: As in NDC OFDM, in I-NDC OFDM also, $(\frac{N}{2} - 1) \log_2 M$ incoming data bits are first mapped to $(\frac{N}{2} - 1)$ QAM symbols, and the input to the N -point IFFT is given by

$$[0, X_1, X_2, \dots, X_{\frac{N}{2}-1}, 0, X_{\frac{N}{2}-1}^*, \dots, X_2^*, X_1^*]^T.$$

This ensures real and bipolar IFFT output. Let $x(n)$, $n = 0, 1, \dots, N - 1$, be the IFFT output. For large N , (e.g., $N \geq 64$), $x(n)$ can be approximated as i.i.d. real Gaussian with zero mean and variance σ_x^2 . Therefore, $|x(n)|$ has an approximately half-normal distribution with mean $\frac{\sigma_x}{\sqrt{2\pi}}$ and variance $\frac{\sigma_x^2(\pi-2)}{2\pi}$ [13]. The IFFT output sequence $x(n)$ is input to a BLOCK selector switch. For each n , $n = 0, 1, \dots, N - 1$, the switch decides the BLOCK to which $x(n)$ has to be sent. This BLOCK selection in a given channel use is done using index bits. Let $b(n)$ denote the index bit for the n th channel use, $n = 0, 1, \dots, N - 1$. The BLOCK selector switch performs the following operation:

$$\begin{aligned} \text{if } b(n) &= 0, & x(n) \text{ goes to BLOCK1} \\ \text{if } b(n) &= 1, & x(n) \text{ goes to BLOCK2.} \end{aligned}$$

In the selected BLOCK, the polarity separator separates positive and negative parts of $x(n)$; $x(n)$ can be written as

$$x(n) = x^+(n) + x^-(n),$$

$$x^+(n) = \begin{cases} x(n), & \text{if } x(n) \geq 0 \\ 0, & \text{if } x(n) < 0, \end{cases} \quad x^-(n) = \begin{cases} x(n), & \text{if } x(n) < 0 \\ 0, & \text{if } x(n) \geq 0. \end{cases}$$

If the selected BLOCK is BLOCK 1, $x^+(n)$ drives LED1 and $-x^-(n)$ drives LED2. Similarly, if BLOCK 2 is selected, $x^+(n)$ drives LED3 and $-x^-(n)$ drives LED4. So, the light intensity emitted by each LED is either $|x(n)|$ or 0. Since $|x(n)| \sim \mathcal{N}_+(\frac{\sigma_x}{\sqrt{2\pi}}, \frac{\sigma_x^2(\pi-2)}{2\pi})$, the intensity I is such that

$$I \in \left\{ \mathcal{N}_+ \left(\frac{\sigma_x}{\sqrt{2\pi}}, \frac{\sigma_x^2(\pi-2)}{2\pi} \right) \right\}.$$

Achieved data rate: In I-NDC OFDM, $(\frac{N}{2} - 1)$ QAM symbols are sent per OFDM symbol. In addition, $\lceil \log_2 N_p \rceil$ number of bits are used to select the active BLOCK per channel use.

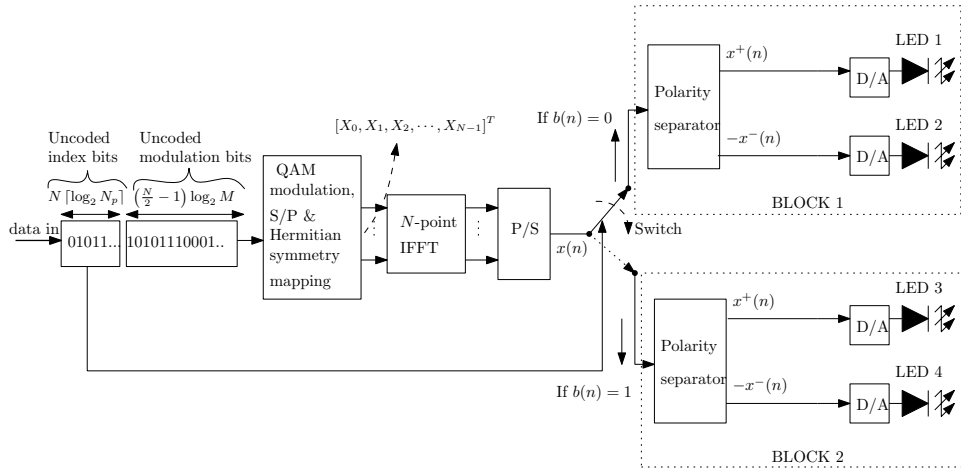


Fig. 5. Proposed I-NDC OFDM transmitter.

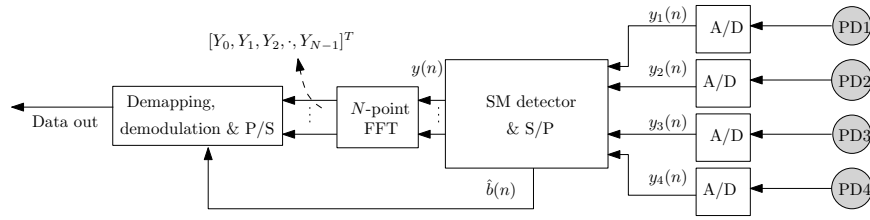


Fig. 6. Proposed I-NDC OFDM receiver.

Therefore, the achieved data rate in I-NDC OFDM is

$$\begin{aligned} \eta_{indc} &= \left(\frac{\frac{N}{2} - 1}{N} \right) \log_2 M + \frac{N \lceil \log_2 N_p \rceil}{N} \\ &= \underbrace{\left(\frac{N-2}{2N} \right) \log_2 M}_{\text{modulation bits}} + \underbrace{\lceil \log_2 N_p \rceil}_{\text{index bits}} \text{ bpcu.} \end{aligned} \quad (11)$$

Receiver: The block diagram of I-NDC receiver is illustrated in Fig. 6. We assume perfect channel state information at the receiver. Assuming perfect synchronization, the $N_r \times 1$ received signal vector at the receiver is given by

$$\mathbf{y} = r\mathbf{H}\mathbf{x} + \mathbf{n}, \quad (12)$$

where \mathbf{x} is the $N_t \times 1$ transmit vector, r is the responsivity of the detector, and \mathbf{n} is the noise vector of dimension $N_r \times 1$. Each element in the noise vector \mathbf{n} can be modeled as i.i.d. real AWGN with zero mean and variance σ^2 . Note that the transmit vector \mathbf{x} has only one non-zero element, and the remaining $N_t - 1$ elements are zeros. The non-zero element in \mathbf{x} represents the light intensity I emitted by the active LED, where $I \sim \mathcal{N}_+(\frac{\sigma_x}{\sqrt{2\pi}}, \frac{\sigma_x^2(\pi-2)}{2\pi})$. The average received signal-to-noise ratio (SNR) is given by $\bar{\gamma} = \frac{r^2 P_r^2}{\sigma^2}$, where

$$P_r^2 = \frac{1}{N_r} \sum_{i=1}^{N_r} \mathbb{E}[\|\mathbf{H}_i \mathbf{x}\|^2] = \frac{\sigma_x^2}{2N_r} \sum_{i=1}^{N_r} \sum_{j=1}^{N_t} h_{ij}^2, \quad (13)$$

and \mathbf{H}_i is the i th row of \mathbf{H} . The received optical signals are converted to electrical signals by the PDs. The output of these

PDs are then fed to the ADCs. The output of the ADCs is given by the vector $\mathbf{y} = [y_1(n) \ y_2(n) \ y_3(n) \ y_4(n)]^T$, which is fed to the SM detector. The bipolar output of the SM detector is fed to the N -point FFT. The SM detector can be a ZF detector. That is, the SM detector output, denoted by $y(n)$, $n = 0, 1, \dots, N-1$, is

$$|y(n)| = \max_{i=1,2,3,4} |z_i(n)| \quad (14)$$

$$\text{sign}\{y(n)\} = \begin{cases} +\text{ve, if } \arg \max_{i=1,2,3,4} |z_i(n)| = 1 \\ -\text{ve, if } \arg \max_{i=1,2,3,4} |z_i(n)| = 2 \\ +\text{ve, if } \arg \max_{i=1,2,3,4} |z_i(n)| = 3 \\ -\text{ve, if } \arg \max_{i=1,2,3,4} |z_i(n)| = 4, \end{cases} \quad (15)$$

where

$$\begin{bmatrix} z_1(n) \\ z_2(n) \\ z_3(n) \\ z_4(n) \end{bmatrix} = \begin{bmatrix} (\mathbf{h}_1^T \mathbf{h}_1)^{-1} \mathbf{h}_1^T \mathbf{y} \\ (\mathbf{h}_2^T \mathbf{h}_2)^{-1} \mathbf{h}_2^T \mathbf{y} \\ (\mathbf{h}_3^T \mathbf{h}_3)^{-1} \mathbf{h}_3^T \mathbf{y} \\ (\mathbf{h}_4^T \mathbf{h}_4)^{-1} \mathbf{h}_4^T \mathbf{y} \end{bmatrix}, \quad (16)$$

and \mathbf{h}_i is the i th column of channel matrix \mathbf{H} , $i = 1, 2, 3, 4$. The SM detector output $y(n)$ is fed to the N -point FFT. The subcarriers 1 to $(\frac{N}{2} - 1)$ at the FFT output and demodulated to get back the transmit data. The index bits $b(n)$ s are detected as $\hat{b}(n) = 0$ if $\arg \max_{i=1,2,3,4} |z_i(n)| = 1$ or 2. $\hat{b}(n) = 1$ if $\arg \max_{i=1,2,3,4} |z_i(n)| = 3$ or 4.

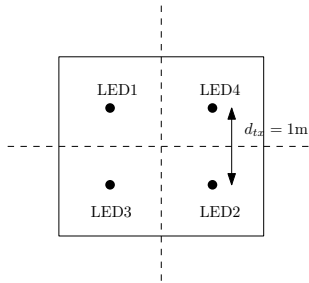


Fig. 7. Placement of $N_t = 4$ LEDs in a 2×2 grid with $d_{tx} = 1\text{m}$.

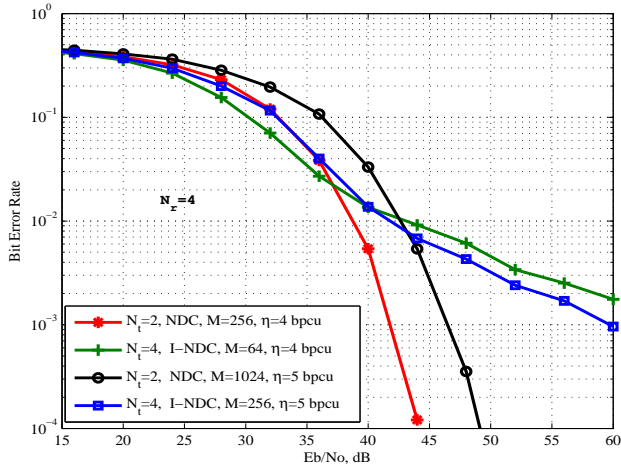


Fig. 8. Comparison of the BER performance of NDC OFDM and the proposed I-NDC OFDM for $\eta = 4, 5$ bpcu, $N_r = 4$.

B. Performance of I-NDC OFDM

Here, we present the BER performance of the proposed I-NDC OFDM scheme for various system parameters. We fix the number of LEDs in I-NDC OFDM to be $N_t = 4$ (see Fig. 5), and the number of PDs to be $N_r = 4$. The placement of $N_t = 4$ LEDs in a 2×2 square grid is shown in Fig. 7. We also compare the performance of the proposed I-NDC OFDM with that of NDC OFDM. LED2 and LED3 are used for NDC OFDM.

Figure 8 presents the BER performance comparison of I-NDC OFDM and NDC OFDM for $\eta = 4, 5$ bpcu. We fix the number of PDs to be $N_r = 4$ for both I-NDC OFDM and NDC OFDM. The parameters considered in these systems for $\eta = 4$ bpcu are: 1) NDC OFDM: $N_t = 2$, $N_r = 4$, $M = 256$, and 2) I-NDC OFDM: $N_t = N_r = 4$, $M = 64$. Similarly, the system parameters considered for $\eta = 5$ bpcu are: 1) NDC OFDM: $N_t = 2$, $N_r = 4$, $M = 1024$, and 2) I-NDC OFDM: $N_t = N_r = 4$, $M = 256$. From Fig. 8, it can be seen that the I-NDC OFDM outperforms NDC OFDM at low SNRs. This is because, to achieve the same spectral efficiency, I-NDC OFDM uses a smaller-sized QAM compared to that in NDC OFDM. But, as the SNR increases, the NDC OFDM outperforms I-NDC OFDM. This is because, as the number of LEDs is increased, the channel correlation increases which affects the detection performance. Note that, though only one LED will be active at a time in both NDC OFDM as well

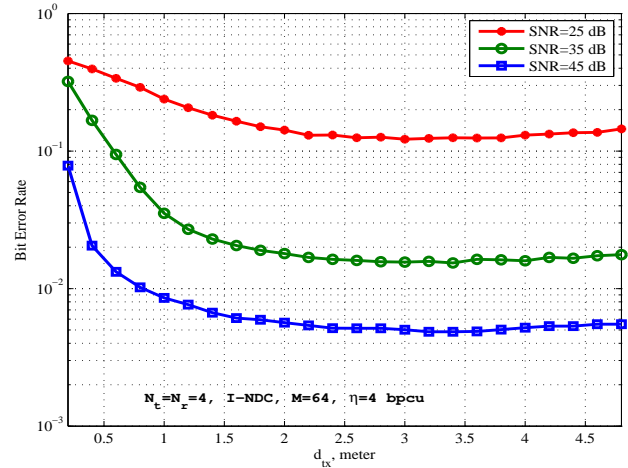


Fig. 9. Comparison of the BER performance of I-NDC OFDM for varying d_{tx} , $\eta = 4$ bpcu, and $N_t = N_r = 4$.

as I-NDC OFDM, NDC OFDM has 2 LEDs whereas I-NDC OFDM has 4 LEDs.

In Fig. 9, we present the BER performance of I-NDC OFDM as a function of the spacing between the LEDs (d_{tx}) by fixing other system parameters. The parameters considered are: $N_t = N_r = 4$, $M = 64$ and $\eta = 4$ bpcu, and SNRs = 25, 35, 45 dB. It is observed from Fig. 9 that there is an optimum d_{tx} which achieves the best BER performance. The optimum spacing is found to be 3.4m in Fig. 9. The BER performance get worse at d_{tx} values those are above and below the optimum spacing. This happens due to opposing effects of the channel gains and the channel correlations. That is, as d_{tx} increases, the channel correlation reduces and which improves the BER performance. On the other hand, the the channel gains get weaker as the d_{tx} increases and this degrades the BER.

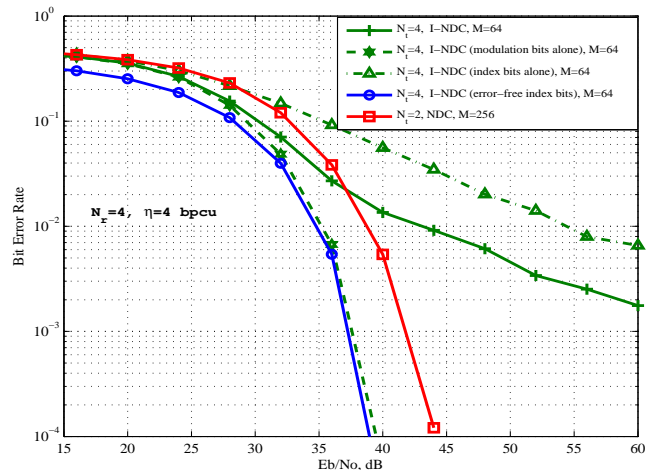


Fig. 10. Reliability of modulation bits and index bits in the proposed I-NDC OFDM for $\eta = 4$ bpcu, $N_r = 4$.

C. Proposed CI-NDC OFDM

Motivation for CI-NDC OFDM: While investigating the poor performance of I-NDC OFDM at high SNRs, we observed from the simulation results that reliability of the index

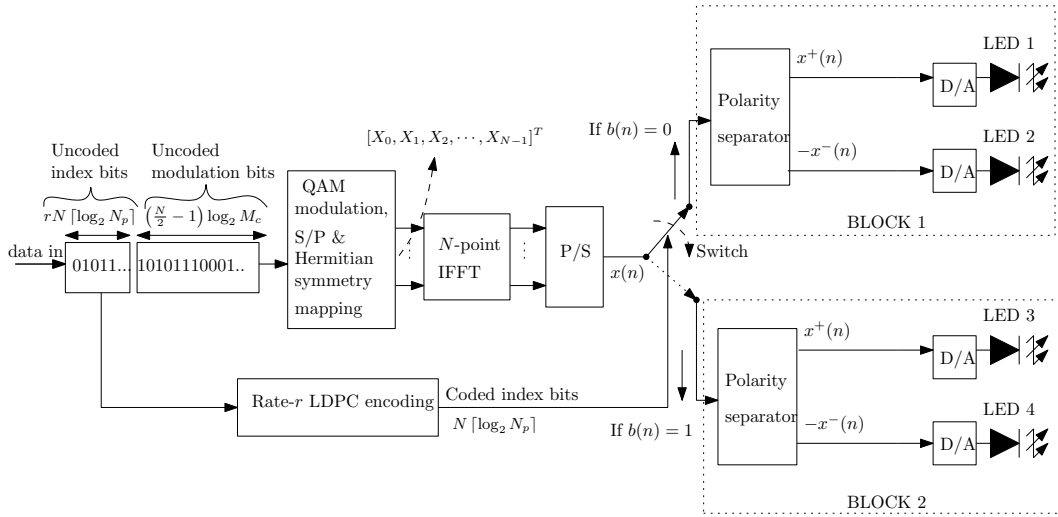


Fig. 11. Proposed CI-NDC OFDM transmitter.

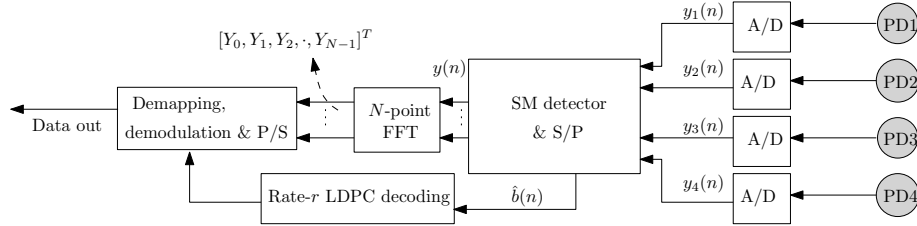


Fig. 12. Proposed CI-NDC OFDM receiver.

bits is far inferior compared to the reliability of the modulation bits. This is illustrated in Fig. 10. As can be seen, the reliability of the index bits is so poor relative to that of the modulation bits, the overall performance is dominated by the performance of the index bits. This is because while the modulation bits have the benefit of OFDM signaling to achieve good performance, the index bits did not have any special physical layer care. This has motivated the need to provide some physical layer protection in the form of coding, diversity, etc. Indeed, as can be seen from Fig. 10, in the ideal case of error-free reception of index bits, the I-NDC OFDM has the potential of outperforming NDC-OFDM even at high SNRs; see the plots of I-NDC OFDM (error-free index bits) and NDC OFDM. Motivated by this observation, we propose to use coding to improve the reliability of index bits.

LDPC coding for index bits: We propose to use a rate- r LDPC code to encode k uncoded index bits and obtain n coded index bits, $r = \frac{k}{n}$. At the transmitter, k_c uncoded index bits are accumulated to obtain n_c LDPC coded index bits. Now, the n_c coded index bits are used to select the index of the active LED block. Thus, one LDPC codeword of size n_c is transmitted in $\frac{n_c}{\lceil \log_2 N_p \rceil}$ channel uses. Therefore, the overall spectral efficiency achieved by the CI-NDC scheme is

$$\eta_{cindc} = r \lceil \log_2 N_p \rceil + \frac{N-2}{2N} \log_2 M_c \text{ bpcu}, \quad (17)$$

where M_c is the size of the QAM alphabet used in CI-

NDC OFDM. The proposed CI-NDC OFDM transmitter and receiver are shown in Figs. 11 and 12, respectively.

D. Performance of CI-NDC OFDM

In Fig. 13, we compare the performance of the proposed C-INDC OFDM with that of NDC OFDM. We match the spectral efficiencies of both the schemes by using the following configurations: 1) NDC OFDM: $N = 64$, $M = 256$, $N_t = 2$, $N_r = 4$, $\eta_{ndc} = 3.875$ bpcu, and 2) C-INDC OFDM: $N = 64$, $M_c = 128$, $N_t = 4$, $N_r = 4$, $r = \frac{1}{2}$, $k_c = 504$, $n_c = 1008$, $\eta_{cindc} = 3.890625$ bpcu. From Fig. 13, we observe that, for the same spectral efficiency of about 3.8 bpcu, the proposed CI-NDC OFDM performs better than NDC OFDM. For example, to achieve a BER of 10^{-5} , CI-NDC OFDM requires about 1.3 dB less SNR compared to NDC OFDM. This is because of the improved reliability of the index bits achieved through coding of index bits.

IV. CONCLUSIONS

We proposed an efficient multiple LED OFDM scheme, termed as coded index non-DC-biased OFDM, for VLC. The proposed scheme was motivated by the high spectral efficiency and performance benefits of using multiple LEDs and spatial indexing. In the proposed scheme, additional information bits were conveyed through indexing in addition to QAM bits. The channel correlation in multiple LED settings was found to significantly degrade the reliability of index bits recovery.

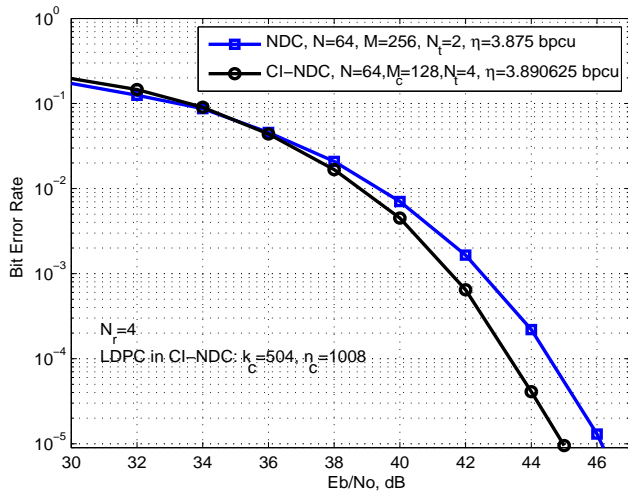


Fig. 13. BER performance of the proposed CI-NDC OFDM and NDC OFDM at $\eta = 3.8$ bpcu, $N_r = 4$.

To overcome this, we proposed coding of index bits. This was found to serve the intended purpose of achieving better performance compared to other OFDM schemes for VLC. Investigation of the proposed signaling architecture for higher-order index modulation using multiple pairs of LEDs can be a topic of further study.

REFERENCES

- [1] J. M. Kahn and J. R. Barry, "Wireless infrared communications," *Proceedings of the IEEE*, vol. 85, no. 2, pp. 265-298, Feb. 1997.
- [2] J. Barry, J. Kahn, W. Krause, E. Lee, and D. Messerschmitt, "Simulation of multipath impulse response for indoor wireless optical channels," *IEEE J. Sel. Areas in Commun.*, vol. 11, no. 3, pp. 367-379, Apr. 1993.
- [3] H. Elgala, R. Mesleh, and H. Haas, "Indoor optical wireless communication: potential and state-of-the-art," *IEEE Commun. Mag.*, vol. 49, no. 9, pp. 56-62, Sep. 2011.
- [4] D. O'Brien, "Visible light communications: challenges and potential," *Proc. IEEE Photon. Conf.*, pp. 365-366, Oct. 2011.
- [5] J. Armstrong, "OFDM for optical communications," *J. Lightwave Tech.*, vol. 27, no. 3, pp. 89-204, Feb. 2009.
- [6] H. Elgala, R. Mesleh, H. Haas, and B. Pricope, "OFDM visible light wireless communication based on white LEDs," *Proc. IEEE VTC 2007-Spring*, pp. 2185-2189, Apr. 2007.
- [7] M. Z. Afgani, H. Haas, H. Elgala, and D. Knipp, "Visible light communication using OFDM," *Proc. IEEE TRIDENTCOM*, Mar. 2006.
- [8] A. H. Azhar, T. A. Tran, and D. O'Brien, "A gigabit/s indoor wireless transmission using MIMO-OFDM visible-light communications," *IEEE Photonics Tech. Letters*, vol. 25, no. 2, pp. 171-174, Dec. 2013.
- [9] A. H. Azhar, T. A. Tran, and D. O'Brien, "Demonstration of high-speed data transmission using MIMO-OFDM visible light communications," *Proc. IEEE GLOBECOM*, pp. 1052-1056, Dec. 2010.
- [10] H. Elgala, R. Mesleh, and H. Haas, "Practical considerations for indoor wireless optical system implementation using OFDM," *Proc. IEEE ConTEL*, pp. 25-29, Jun. 2009.
- [11] D. Tsonev, H. Chun, S. Rajbhandari, J. J. D. McKendry, D. Videv, E. Gu, M. Haji, S. Watson, A. E. Kelly, G. Faulkner, M. D. Dawson, H. Haas, and D. O'Brien, "A 3-Gb/s single-LED OFDM-based wireless VLC link using a gallium nitride μ LED," *IEEE Photonics Tech. Lett.*, vol. 26, no. 7, pp. 637-640, Jan. 2014.
- [12] O. Gonzalez, R. Prez-Jimnez, S. Rodriguez, J. Rabadn, and A. Ayala, "OFDM over indoor wireless optical channel," *Proc. IEE Optoelectronics*, vol. 152, no. 4, pp. 199-204, Aug. 2005.
- [13] J. Armstrong and A. J. Lowery, "Power efficient optical OFDM," *Electronics Letters*, vol. 42, no. 6, pp. 370-372, Mar. 2006.
- [14] J. Armstrong and B. J. Schmidt, "Comparison of asymmetrically clipped optical OFDM and DC-biased optical OFDM in AWGN," *IEEE Commun. Letters*, vol. 12, no. 5, pp. 343-345, May 2008.
- [15] J. Armstrong, B. J. Schmidt, D. Kalra, H. Suraweera, and A. J. Lowery, "Performance of asymmetrically clipped optical OFDM in AWGN for an intensity modulated direct detection system," *Proc. IEEE GLOBECOM 2006*, pp. 1-5, Nov. 2006.
- [16] N. Fernando, Y. Hong, and E. Viterbo, "Flip-OFDM for optical wireless communications," *Proc. IEEE ITW 2011*, pp. 5-9, Oct. 2011.
- [17] N. Fernando, Y. Hong, and E. Viterbo, "Flip-OFDM for unipolar communication systems," *IEEE Trans. Commun.*, vol. 60, no. 12, pp. 3726-3733, Aug. 2012.
- [18] Y. Li, D. Tsonev, and H. Haas, "Non-DC-biased OFDM with optical spatial modulation," *Proc. IEEE PIMRC 2013*, pp. 486-490, Sep. 2013.
- [19] F. R. Gfeller and U. Bapst, "Wireless in-house data communication via diffuse infrared radiation," *Proceedings of the IEEE*, vol. 67, no. 11, pp. 1474-1486, Nov. 1979.